Optica Applicata, Vol. XXXIV, No. 1, 2004

Computer simulation of modulated two-beam interference using monochromatic light

A.M. HAMED

Physics Department, Faculty of Science, Ain Shams University, Cairo, Egypt,
e-mail: amhamed73@hotmail.com

Two different models are suggested to describe the fringe shift obtained from the two beam interference modulated by the phase variations of transparent objects. The first model of the fringe shift assumes a linear triangular distribution, while the second model varies as a truncated Gauss function. The Abel transform enables computation of the refractive index distribution from the theoretical data of the fringe shift. The fringe shift of the phase object is represented in the harmonic term of the intensity distribution formula. A computer program is written to plot both of the fringe shifts of the models described and the corresponding refractive indices of the phase object. Comparative results are cited in the introduction which are based on an algebraic reconstruction technique (ART) using two models; one of them has a cosine phantom field which constructs an asymmetric single peak, while the other model has cosGauss function giving an asymmetric double-peak phantom. These results are compared with our results, which gives only a single peak in both cases of linear and quadratic variations, which is convenient for use in optical fibers.

Keywords: apodized apertures, amplitude modulation, two-beam interference, Abel transform.

1. Introduction

Over the years, many different techniques have been used to measure quantitatively the refractive index distribution of inhomogeneous media [1]–[14]. Among these are interference methods which have been used for index measurements of thin films [15] and optical fibers [16]. It has been shown that low-coherence interferometer is best suited for measurements of thickness and index of refraction [17]. Methods based on Fourier transform techniques [18] applied to speckle images and other methods based on Abel transform techniques [19], [20] were used to compute refractive index distribution from the measurement of light deflection [21], [22]. Also, methods based on recording projections to measure phase variations in transparent biological 3D objects have been investigated [23]. The method allowed us to reconstruct, plane by plane, a map of variation of phase or refractive index making use of transverse tomography [24], [25]. Recently, Fourier transform techniques and Abel deconvolution are used to analyze a finite fringe holographic interferogram produced by an

axisymmetric shock wave flow to draw a density map that can be compared with a numerical model [26]. In general, interferometry, using different techniques including Mach–Zehnder, Michelson, and holographic interferometers, has been very useful for providing data against which computational fluid dynamic simulation can be compared. In particular, holographic interferometry is useful for density measurements in flow produced by shock waves [27]. Also, a recent publication utilizing an optical method based on speckle photography to measure the refractive index gradients [28] of a phase object has been presented. It measures the amount of dislocation of optical speckles that linearly increases with an increasing refractive index gradient at the measurement point. The measured refractive index gradients are then converted into the medium temperature and density information using pertinent physical equations. An improved technique for determining the change in the refractive index of bulk glass samples [29] using Michelson interferometer has been presented. This method uses a Michelson arrangement in order to characterize the induced index change in bulk glass and optical fiber preforms. Another research work on speckle interferometry was found to be easier than speckle photography in some applications for direct temperature measurements [30]. The speckle photography provides only the gradient of refractive index, while speckle interferometry gives complete information on refractive index itself. A different method based on mathematical inversion procedure for speckle photography has been developed using the 2D Fourier transformation. This method is called Fourier convolution (FC) [31] which is considered to be a simple method but suffers from reduced reconstruction accuracy when the amount of projection data is limited.

A research work using algebraic algorithm reconstruction technique (ART) was developed for the purpose of using tomographic reconstruction of density-gradient optical projection method. The extended ART [32]–[34] was numerically tested by using two models; one of them has a cosine phantom field which constructs an asymmetric single peak while the second model has a cosGauss function which gives an asymmetric double-peak phantom. The extended ART converts the non-algebraic speckle projections data into algebraic interferometric projections so that the conventional ART iteration can proceed.

In this paper, we propose a simple method to recover 3D refractive index distribution of phase objects from the local differential fringe shift of the proposed linear and quadratic models as compared with the above method that uses a digitizing oscilloscope for recording the optical path difference in order to measure the induced index changes in the bulk glass [29] using Michelson interferometer. The motivation for the selection of these models, cited in the abstract, lies in their resemblance with the fringe shift occurring due to the introduction of phase object, like optical fibers, in one of the arms of the interferometer. A triangular model is suggested as a linear variation function, while quadratic shift variation represented by a truncated Gauss function is set to represent the graded index fibers. Hence, these models are considered

most suitable to describe phase shifts introduced by optical fibers. In the following section, a theoretical analysis is presented based on two beam interference considering monochromatic light for the illumination of the interferometer. A method of calculation of the refractive index from the fringe shift, based on Abel transform, is presented followed by a discussion of the results and conclusions.

2. Theoretical analysis

A Michelson arrangement illuminated with monochromatic light is used as a processor, as shown in Fig. (1). The phase object examined is placed in one of the arms of the interferometer, while an inclined plane wave, making an angle α with respect to the normal working as a carrier wave is incident upon the second arm of the interferometer. In the imaging plane of coordinates (y, z), the recorded intensity is represented by the well known expression of the two beam interference as follows [35]:

$$I(y, z) = 4\gamma\beta_1 \cos^2\left[\frac{\Phi_0}{2} - \frac{\pi}{\lambda} y \sin\alpha\right] \tag{1}$$

where $\gamma = a^2(\lambda)$ is characteristic of the illumination of the interferometer and $\beta_1 = \beta_2 = T_s R_s R_1$ is dependent upon the optical components of the interferometer, namely

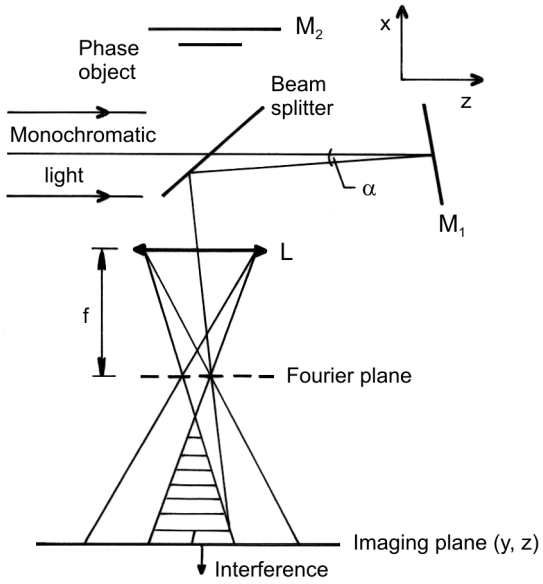

Fig. 1. Two-beam interference using monochromatic light, where a phase object of thickness t_p is introduced in the arm containing the mirror M_2, α is the oblique angle made between the mirror M_1 and the reflected ray, L is the imaging lens.

the beam splitter and the mirrors M_1, M_2 (R_s, T_s – the intensity reflection and transmission coefficients of the beam splitter, and R_1 – the intensity reflection coefficient of the mirror M_1).

The phase variation Φ_o is related to the optical path difference (OPD) as follows:

$$\Phi_0(y, \lambda) = \frac{2\pi}{\lambda}(\mathrm{OPD}) = \frac{2\pi}{\lambda}\{2[n(y) - 1]t_p\} \tag{2}$$

where t_p is thickness of the phase object and $n(y)$ represents the refractive index variations.

3. Special cases

3.1. Triangular model for the fringe shift

It utilizes an inhomogeneous phase object of constant thickness t_p but of variable refractive index. The variation is represented by a triangular function given by

$$n(y) = \begin{cases} n_0\left[1 - \left|\dfrac{(y - y_0)}{b}\right|\right] & \text{for} \quad |y| \le b \\ 1 & \text{for} \quad |y| > b \end{cases} \tag{3}$$

where n_0 is the maximum refractive index located at the center of the pattern, y_0 represents the shift introduced at a certain depth z, and b is the width of the triangular shape.

From Eq. (1), Eq. (3) and using Eq. (2), we get

$$I(y, z) = 4a^2(\lambda)T_s R_s R_1 \cos^2\left\{\frac{\pi}{\lambda}\left[y \sin\alpha - 2(n(y) - 1)t_p\right]\right\} \tag{4}$$

where the phase of the object is calculated for the triangular object as

$$\Phi_0(\lambda) = \frac{2\pi}{\lambda}\{2[n(y) - 1]t_p\} = \frac{2\pi}{\lambda}\Delta s. \tag{5}$$

In order to compute the fringe shift introduced by the phase object, we firstly calculate the fringe spacing Δz from the difference between the maximum intensities of two consecutive fringes, using Eq. (4), and we obtain [35]

$$\Delta z = \frac{\lambda}{\sin\alpha}. \tag{6}$$

In this case, since α is a small angle, then it is rewritten approximately as follows:

$$\Delta z = \frac{\lambda}{2\sin(\alpha/2)}. \tag{6a}$$

Assuming that the shift introduced by the phase object is less than the interfringe spacing, *i.e.*, $\Delta s < \Delta z$, then we can write this inequality, using Eq. (5), and Eq. (6a), as follows:

$$t_p < \frac{\lambda}{4[n(y)-1]} \sin\left(\frac{\alpha}{2}\right). \tag{7}$$

where $n(y)$ is given by Eq. (3).

Since $m\lambda$ = OPD, for constructive interference, m is the order of interference. Hence, substituting Eq. (3) in the above equation, the fringe shift may be calculated from the equation of straight line fringes modulated by a triangular fringe shift as follows :

$$m\lambda = \begin{cases} y\sin\alpha - 2\left[n_0\left(1-\left|\frac{y}{b}\right|\right)\right]t_p - \frac{2n_0y_0t_p}{b} + 2t_p & \text{for} \quad |y| \le b \\ y\sin\alpha & \text{for} \quad |y| > b \end{cases}. \tag{8}$$

If this condition is fulfilled $n_0y_0 = b$ (*e.g.*, take $n_0 = 1.5$ and $b/y_0 = 1.5$). In this case, Eq. (8) becomes

$$m\lambda = y\sin\alpha - 2\left[n_0\left(1-\left|\frac{y}{b}\right|\right)\right] \quad \text{for} \quad |y| \le b. \tag{9}$$

Consequently, the differential fringe shift becomes

$$D_z(y) = \frac{\Delta s}{\Delta z} = 4n_0\left(1-\left|\frac{y}{b}\right|\right)\frac{t_p}{\lambda}\sin\frac{\alpha}{2}. \tag{10}$$

It represents an exact triangular function for the cited model and Δz is the interfringe spacing calculated from Eq. (6a).

3.2. Truncated Gauss model for the fringe shift

A truncated Gauss function is assumed to represent the fringe shift obtained in the case of two-beam interference. Inhomogeneous phase object of a refractive index $n(y)$ is assumed to have a shifted Gauss function, *i.e.*,

$$n(y, \lambda) = n_0 \exp\left\{-\beta\left[\frac{y - y_0}{w}\right]^2\right\} \quad \text{for} \quad |y| \le w \tag{11}$$

where w is the truncation width, β is a parameter, and y_0 represents the shift introduced at a certain depth z.

In this case, the intensity distribution is similar to Eq. (4) except that the refractive index is represented by Eq. (11). The straight-line fringes are modulated by Gauss function that represents the shift proposed as

$$m\lambda = y\sin\alpha - 2\left\{n_0 \exp\left\{-\beta\left[\frac{y - y_0}{w}\right]^2\right\} - 1\right\} t_p. \tag{12}$$

The shift y_0 may be compensated with the linear shift t_p leading to an exact Gauss distribution for the fringe shift. Hence, the differential fringe shift is calculated as:

$$D_z(y) = \frac{\Delta s}{\Delta z} = 2\left\{n_0 \exp\left[-\beta\left(\frac{y}{w}\right)^2\right]\right\} \frac{t_p}{\lambda} \sin\left(\frac{\alpha}{2}\right). \tag{13}$$

4. Method of calculation

The back substitution simulation process is used to map the refractive index distribution from the fringe shifts described by the above models. The solution is based on the Abel transformation of the theoretical data. It is commode to cite that the transformation occurs in the same plane at a certain depth z. The Abel integral is explicitly written as [19]

$$D_z(y) = \frac{1}{\lambda} \frac{\int [n(r) - n_0] \mathrm{d}r^2}{(r^2 - y^2)^{1/2}} \tag{14}$$

where n_o is the refractive index outside the inhomogeneous phase object. This integral is approximated by the following summation:

$$D_j = \frac{1}{\lambda} \sum_{i=j}^{N} \Psi(j, i) f_i. \tag{15}$$

The matrix of coefficients $\Psi(j, i)$ is reduced to the matrix summation of elements [10]

$$\Psi(j, i) = 2h\{[i^2 - (j-1)^2]^{1/2} - [(i-1)^2 - (j-1)^2]^{1/2}\} \tag{16}$$

where h is the zone width.

The phase object of maximum radius R_m is subdivided into N zones of width h, where $0 = r_0 < r_1 < r_2 < \ldots < r_{N-1} < r_N = R_m$, $|r_j - r_{j-1}| = h$, $j \le i \le N$. The recursive solution of the system of equations for f_j is written as follows [10]:

$$f_j = \frac{1}{2h(2j-1)^{1/2}} \left[\lambda D_j - \sum_{i=j+1}^{N} \Psi(j, i) f_i \right] \tag{17}$$

If the index values f_i (with $j + 1 < i < N$) are known, one may determine the values f_j. Hence, for arbitrary value of $r = (y, z)$ one may derive the refractive index n by linear interpolation between the respective values $n(r_j)$ and $n(r_{j-1})$ if $r_j > r > r_{j-1}$. Hence,

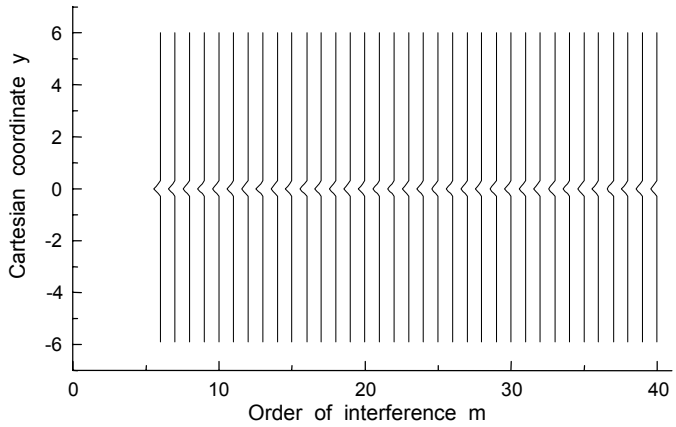

Fig. 2. Straight line interference fringes modulated by a triangular fringe shift corresponding the triangular model.

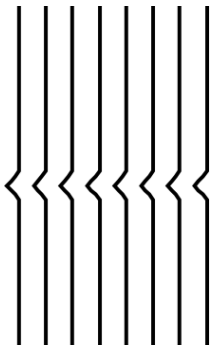

Fig. 3. Magnified portion of eight fringes modulated by triangular fringe shift Δs.

the solution of the system of linear equations represented by Eq. (17) is obtained using the back-substitution and Gauss elimination processes [36].

5. Results and discussion

A computer program is constructed to map the straight line fringes obtained from the two beam interference modulated by the fringe shifts models. The first model of triangular function is plotted as in Fig. 2, where 35 fringes are plotted and the modulation of triangular function is centered symmetrically around the *z*-axis. A magnified portion of only eight fringes is plotted in Fig. 3. The corresponding refractive index computed from Eq. (10) and Eq. (17) is shown in Fig. 4. It is shown that the refractive index distribution of the phase object has the same shape as the proposed model of triangular distribution. The second model of truncated Gauss function is plotted as in Fig. 5 and the corresponding refractive index distribution computed from Eq. (13) and Eq. (17) is plotted as in Fig. 6 which is in good agreement with the Gauss model. It follows from these results that the distribution of the refractive indices is similar to the aforementioned models of the fringe shifts and this may be attributed to the imaging interference manipulation. The theoretical curves of refractive indices are computed from the back-substitution simulation process as stated in the section on the method of calculation. The method of extraction of the 3D refractive index of phase objects from the fringe shift may be extended to process arbitrary refractive indices. In this case, sampling process is needed to obtain the required data from the fringe shift. The phase encoding of the object is obtained from the fringe shift by using the interferometer of Michelson.

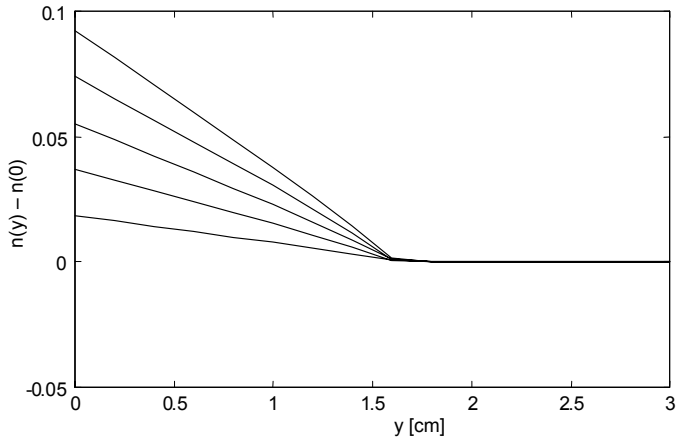

Fig. 4. Theoretical contour mapping of the refractive index *vs.* Cartesian coordinate *y* using a triangular input function.

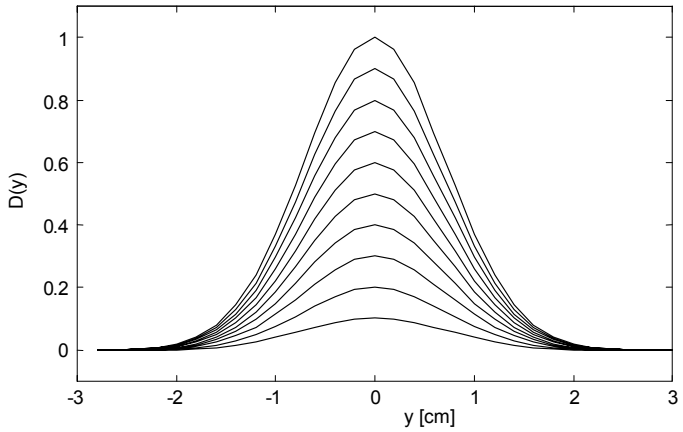

Fig. 5. Truncated Gauss function used as an input data for the processing of the refractive index distribution of the phase object.

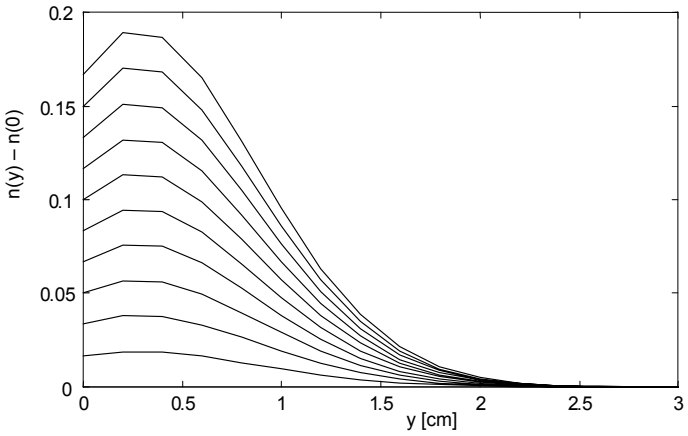

Fig. 6. Theoretical contour mapping of the refractive index using a truncated Gauss function for the input data.

The interferometer is illuminated by a carrier wave that emitted from a He-Ne laser beam.This carrier wave interferes with the object wave that carries amplitude and phase information. Hence, phase encoding is formed in the imaging plane.

6. Conclusions

We have suggested two different models to describe the fringe shifts introduced in the phase term appearing in the intensity distribution formula. In this study, a two-beam

interference is considered using the arrangement of Michelson introducing the phase object in one of the arms of the interferometer. A triangular and Gauss profiles are chosen as models to represent the fringe shifts that resemble the phase shift produced by optical fibers. The corresponding refractive indices are computed from the differential fringe shifts of the models using back-substitution process. The potential of the research presented is suitable to process arbitrary phase objects. It requires 2D sampling of the object to put it in a matrix form. Then, the back-substitution process is applied to this arbitrary phase object. Also, this simulation process may be extended to process the coloured-phase objects using polychromatic light for the illumination of the interferometer. This polychromatic spatially coherent light may be obtained by mixing He-Ne laser and argon ion laser for the illumination of the interferometer [37]. One of the advantages of this method as compared with computer tomography (CT) based on Fourier convolution (FC) of images lies in its relative simplicity, since the former method needs only a simple Abel transformation, while the FC method requires a lot of time for computing the CT as it requires computing Fourier transformations and convolution operations.

References

[1] KOPF U., Opt. Commun. **5** (1972), 347.
[2] SHU J.Z., LI I.Y., J. Flow Visual Image Process. **1** (1993), 63.
[3] MERZKIRCH W., Exp. Therm. Fluid Sci. **10** (1995), 435.
[4] KIHM K.D., Exp. Fluids **17** (1994), 246.
[5] WALSH T.E., KIHM K.D., J. Flow Visual. Image Process. **2** (1995), 299.
[6] Merzkirch W., *Density – sensitive whole – field flow measurement by optical speckle photography*, Proc. Int. Conf. Exp. Heat Transfer, Fluid Mech. Thermodyn. 3rd, Honolulu, Hawaii, (1993) pp. 1–11.
[7] LIU T.C., MERZKIRCH W., OBERSTE-LEHNE K., Exp. Fluids **7** (1989), 157.
[8] ERBECK R., MERZKIRCH M., Exp. Fluids **6** (1988), 89.
[9] MICHAEL Y.C., *Three-dimensional temperature reconstruction using Mach–Zehnder interferometric tomography*, Ph. D. Thesis, Department of Aerospace and Mechanical Engineering, University of Notre Dame, South Bend, USA, 1991.
[10] BARAKAT N., EL-GHANDOOR H., HAMED A.M., DIAB S., Exp. Fluids **16** (1993), 42.
[11] LIRA I.H., Meas. Sci. Technol. **5** (1994), 226.
[12] RADULOVIC P.T., *Holographic interferometry of three-dimensional temperature of density fields*, Ph. D. Thesis, Department of Mechanical Engineering and Applied Mechanics, University of Michigan, Ann Arbor, USA, 1977.
[13] FOMIN N.A., Inzh.-Fiz. Zh. **56** (1989), 540.
[14] BLINKHIN G.N., FOMIN N.A., ROLIN M.N., SOLOUKHIN R.L., VITKIN D.E. YADREVSKAYA N.L., Exp. Fluids **8** (1989), 72.
[15] FUKANO T., YAMAGUCHI I., Opt. Lett. **21** (1996), 1942.
[16] CANNING A.L., CARTER G., SCEATS M.G., J. Lightwave Technol. **15** (1997), 1348.
[17] FLOURNOY P.A., MCCLUE R.W., WYNTJES G., Appl. Opt. **11** (1972), 1907.
[18] BUTTERS J.N., LEENDERTZ J.N., J. Phys. **E4** (1971), 277.
[19] BRACEWELL R.N., *The Fourier Transform And Its Applications*, McGraw-Hill Co., New York 1978, p. 261.

[20] VEST C.V., *Holographic Interferometry*, Wiley, New York 1979.
[21] SHU J.Z., LI J.Y., J. Flow Visualization Image Processing **1** (1993), 63.
[22] WERNEKINCK U., MERZKIRCH W., FOMIN N.A., Exp. Fluids **3** (1985), 206.
[23] VONBALLY G., *Holography in medicine and biology*, Proceedings of the International workshop, Munster, Fed.Rep. Germany (1979) p. 124.
[24] WALSH T.E., KIHM K.D., *Tomographic deconvolution of laser speckle photography applied for flame temperature measurement*, Proc. Int. Symp. Flow Visual. 7th Seattle, 1995, pp. 898–903.
[25] WALSH T.E., *A comparative study of laser speckle photography and laser interferometry for optical tomography*, Ph. D. Thesis, Department of Mechanical Engineering, Texas A&M University, College station, TX, USA, 1996.
[26] HOUWING A.F.P., TAKAYAMA K., KOREMOTO K., HASHIMOTO T., FALETIC R., GASTON M., *Interferometric measurement of an axi-symmetric density field*, 2nd Australian Conference on Laser Diagnostics in Fluid Mechanics and Combustion, Monash University, Melbourne, Australia, 9–10 Dec., 1999, pp. 111–116.
[27] TAKAYAMA K., Proc. Soc. Photo-Opt. Instrum. Eng. **398** (1983), 171.
[28] KIHM K.D., Opt. Lasers Eng. **29** (1998), 171.
[29] TASSHI D., ERIN M. GILL, SARAH L.G., Appl. Opt. **40** (2001), 1663.
[30] SHAKHER C, NIRALA A.K., Optik **97** (1994), 43.
[31] LIU T.C., MERZKIRCH M., OBERSTE-LEHAN K., Exp. Fluids **7** (1989), 157.
[32] GORDON R., IEEE Trans. **NS-21** (1974), 78.
[33] VERHOEVEN D., Appl. Opt. **32** (1993), 3736.
[34] KO H.S., KIHM K.D., Exp. Fluids **27** (1999), 542.
[35] LIPSON S.G., LIPSON H., TANNHAUSER D.S., *Optical Physics*, 3rd ed., Cambridge 1996, p. 222.
[36] CHAPRA S.C., CANALE R.P., *Introduction to Computing for Engineers*, Mc-Graw Hill Co. (1986), p. 496.
[37] HAMED A.M., Opt. Appl. **13** (1983), 205.

Received June 10, 2002
in revised form August 11, 2003